Electrochemical Determination of Indole-3-carboxylic Acid Using Carboxyl Functionalized Multi-Walled Carbon Nanotubes Modified Glassy Carbon Electrode

X.L. Jia[1], J.H. Ye[1], F.Q. Wang[1], Y.L. Hu[1], M.Z. Zheng[1], C.Z. Wu[1,2,*]

[1] Fujian Provincial Key Laboratory of Eco-Industrial Green Technology, Wuyi University, Wuyishan 354300 China.
[2] College of Life Science, Fujian Agriculture and Forestry University, Fuzhou, 350002, China.
[*]E-mail: fjwcz@126.com

Indole-3-carboxylic acid (ICA) was detected by differential pulse voltammetry using a glassy carbon electrode (GCE) modified carboxylic multi-walled carbon nanotubes (MWCNTs-COOH). Electrochemical impedance spectroscopy (EIS) and different pulse voltammetry (DPV) were used to study electrochemical properties of the modified electrode. The modified electrode shows higher electrocatalytic activity toward the oxidation of Indole-3-carboxylic acid than those of the carbon electrode modified multi-walled carbon nanotubes or bare glassy carbon electrode. After the experimental conditions were optimized, the linear calibration curve was obtained in the range from 0.75 to 100 $\mu mol\cdot L^{-1}$ with a low detection limit of 0.25 $\mu mol\cdot L^{-1}$ (S/N = 3). The modified electrode was successfully used for the determination of the analytes in real samples, which obtained satisfactory results.

1. INTRODUCTION

Plant hormone as a kind of physiological activity substance can adjust plant growth effectively and determine most properties of the plant at their low concentrations. And indole carboxylic acids belonging to the auxins family is well-known. Indole-3-carboxylic acid (ICA) [1] is one of components in the decarboxylative pathway that has been identified as an endogenous constituent in higher plants on the basis of strict physicochemical evidence [2]. And ICA also is the metabolites of indole-3-acetic

acid (IAA). The catabolism of IAA to ICA may be one of mechanisms by which ethylene reduces endogenous IAA levels [3]. Thus, the measurement of ICA seems to be quite important. The most common method of determination of ICA was reversed-phase liquid chromatography[1, 4], However, organic solvents are generally used as the mobile phase, which is not a green approach. HPLC method also suffers from the disadvantages of complex instruments and being time-consuming.

Indoleamine hormone possesses unsaturated heterocyclic moiety which provide a chance for the determination of indoleamine hormone by electrochemical methods. Unfortunately, the electrochemical activity of indoleamine hormone is rather weak [5]. Recently, some efforts have successfully been made to determine IAA [6-8]. As ICA has one fewer methylene than IAA, it is difficult to be oxidized by single electron compared with that of IAA. Therefore, the electrochemical oxidation of ICA is especially difficult.

Carbon nanotubes (CNTs) have been widely utilized for the modification of electrodes due to their high chemical stabilities, high surface areas and unique electronic properties in the last decade [9-11]. However, the pristine CNT flocculate rapidly in aqueous or common organic solutions, hindering their further manipulations and applications [12]. CNTs functionalized with groups such as carboxylates have negative charges, which make the CNTs repel each other and keep the solution dispersed [13]. Carboxylic multi-walled carbon nanotubes (MWCNTs-COOH) can improve the hydrophilicity of carbon nanotubes, making it easier to disperse into DMF to prepare a uniform electrode film [14]. In this paper, electrochemical properties of ICA were studied on the MWCNTs-COOH modified glassy carbon electrode (MWCNTs-COOH/GCE). On this basis, an electrochemical sensor for the determination of ICA using MWCNTs-COOH/GCE was developed.

2. EXPERIMENT

2.1 Apparatus

Electrochemical measurements was carried out by a CHI660D Electrochemical Workstation (Shanghai Chenhua Instruments, Shanghai, China) combined with the classical three-electrode system. An Ag/AgCl electrode containing a KCl saturated solution, a platinum electrode and a bare GCE or MWCNTs-COOH/GCE were employed as reference electrode, auxiliary electrode and working electrode, respectively.

2.2 Chemicals

The MWCNTs were obtained from Chengdu Institute of Organic Chemistry, Chinese Academy of Sciences. ICA was purchased from the Chinese Institute of Biological Products Control (Beijing, China). Other reagents involved were analytical grades. Phosphate (PP) buffer solution was prepared by mixed 0.2 mol L^{-1} Na_2HPO_4 / 0.2 mol L^{-1} NaH_2PO_4 solutions with different volume ratios. Distilled water was used for solution preparation and washing. Both standard solutions and buffer solutions were stored at 4 ∘C.

2.3 Preparation of MWCNTs-COOH

MWCNTs were treated and functionalized according to previously described literature [15]. 20 g of MWCNTs and 200 mL of 30% H_2O_2 solution were mixed in a 250 mL glass flask. The mixtures were stirred for 1 h and then 10 mL of 0.6 mol mL^{-1} H_2SO_4 was added to the black suspension. And which was refluxed for 1 h at 105 ∘C. Finally, the mixed solution obtained was vacuum-filtered through 0.2 μm Millipore polytetrafluoroethylene membrane and washed with distilled water until the pH of the filtrate was 7.0. The filtered solid was dried in a vacuum oven at 60 ∘C for 24 h to obtain the MWCNTs-COOH.

2.4. Preparation of MWCNTs-COOH/GCE

For preparation of the MWCNTs-COOH/GCE, a bare GCE was firstly polished the surface of the electrode using a polishing cloth with 0.05 μm alumina slurry. Afterwards, the surface of the electrode was rinsed thoroughly with distilled water. The aforementioned electrode was then ultrasonically oscillated in ethanol and double-distilled water for 5 min, respectively. Finally, cyclic potential sweeping was conducted for the above-electrode with scanning potential range of -0.20 and 1.50 V in 0.5 mol·L^{-1} H_2SO_4 solution until a stable cyclic voltammogram was obtained. The pretreatment for bare GCE was completed. Subsequently, 1 mg of MWCNTs-COOH was added into 1 mL of DMF solvent and then ultrasonically oscillated for 30 min to form the MWCNTs-COOH suspension. After that, 10 μL of as-prepared suspension was pipetted onto the surface of GCE and the solvent was evaporated at room temperature in the air. This electrode was denoted as MWCNTs-COOH/GCE. The MWCNTs/GCE was also fabricated following a similar procedure.

3. RESULTS AND DISCUSSION

3.1. Electrochemical characterization of different modified electrodes

Electrochemical impedance spectroscopy (EIS) and cyclic voltammetry (CV) methods were used to study the electrochemical behaviors of different modified electrodes. The measurements were performed in a mixed solution which contained 0.1 mol·L^{-1} KCl and 5.0 mmol·L^{-1} $K_4[Fe(CN)_6]/K_3[Fe(CN)_6]$.

The Nyquist plots of different modified electrodes are shown in Fig. 1. For bare GCE (curve a), a typical semicircle is presented at the beginning of the impedance plot and a 45° Warburg diffusion line can be observed subsequently (curve a). These phenomenon display that the electrochemical reaction of $K_4[Fe(CN)_6]/K_3[Fe(CN)_6]$ on the bare GCE is kinetically controlled at high frequencies and diffusion controlled at low frequencies [17]. However, the diameter of semicircle for MWCNTs-GCE decrease obviously compared with bare GCE, suggesting that the electron-transfer process of

$K_4[Fe(CN)_6]/K_3[Fe(CN)_6]$ can be promoted due to the good conductivity and high specific surface area of the MWCNTs.
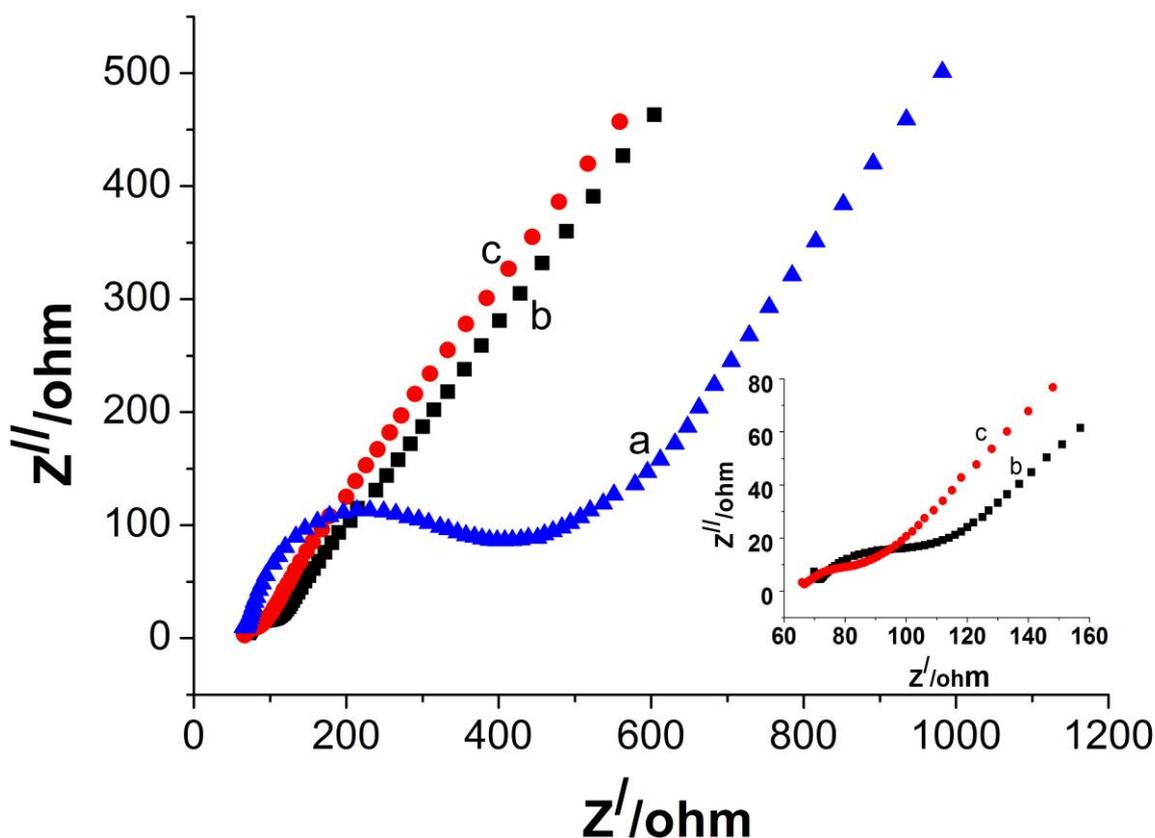
Figure 1. EIS curves of electrode in 5.0 mmol·L^{-1} $K_4[Fe(CN)_6]/K_3[Fe(CN)_6]$ (1:1) solution containing 0.1 mol·L^{-1} KCl: (a) GCE, (b) MWCNTs/GCE, (c) MWCNTs-COOH /GCE

Ac voltage: 5 mV; Frequency range: 0.1 – 10 MHz

After coating with the MWCNTs, the diameter of the semicircle (curve b) decrease obviously suggesting that the MWCNTs film can promote the electron-transfer process. When the surface of GCE was modified with MWCNTs-COOH, the smallest semicircle was obtained (curve c). The MWCNTs-COOH/GCE has a very small interfacial electron transfer resistance. This phenomenon indicates that MWCNTs-COOH can decrease the resistance of the electrode. These results also demonstrate that MWCNTs-COOH is successfully immobilized on the GCE surface.The MWCNTs-COOH forms a good electron channel between the electrode surface and electrolyte, accelerating the electron transport of $K_4[Fe (CN)_6]/K_3[Fe (CN)_6]$ on the surface of solution and electrode.

Cyclic voltammetry (CV) can provide useful information on the barrier changes of the electrode surface during the fabrication process. Fig. 2 shows the CVs of bare GCE, MWCNTs/GCE and MWCNTs-COOH/GCE. Well-defined oxidation and reduction peaks corresponding to $K_4[Fe(CN)_6]/K_3[Fe(CN)_6]$ couple are observed at bare GCE (curve a). The peak-to-peak separation (ΔE_p) value is 0.121 V. Compared to bare GCE, the ΔE_p of MWCNTs/GCE (curve b) decreases to

0.108 V and the redox peak currents also increases. This result indicates that MWCNTs film formed on the electrode surface is a good conductive media to facilitate the interfacial electron transfer.

According to the view of Hrapovic and Yang[23-24], the larger surface area of the electrode is, the better the electrocatalytic performance and the higher the sensitivity will be.

If the MWCNTs-COOH/GCE is used in this system, not only the redox peak currents can be significantly improved, but also the ΔE_p (0.099 V) would substantially become narrow. This phenomenon suggests that MWCNTs-COOH has excellent electrical conductivity and fast electron transfer rate due to its large surface area. These results are consistent with the EIS data.
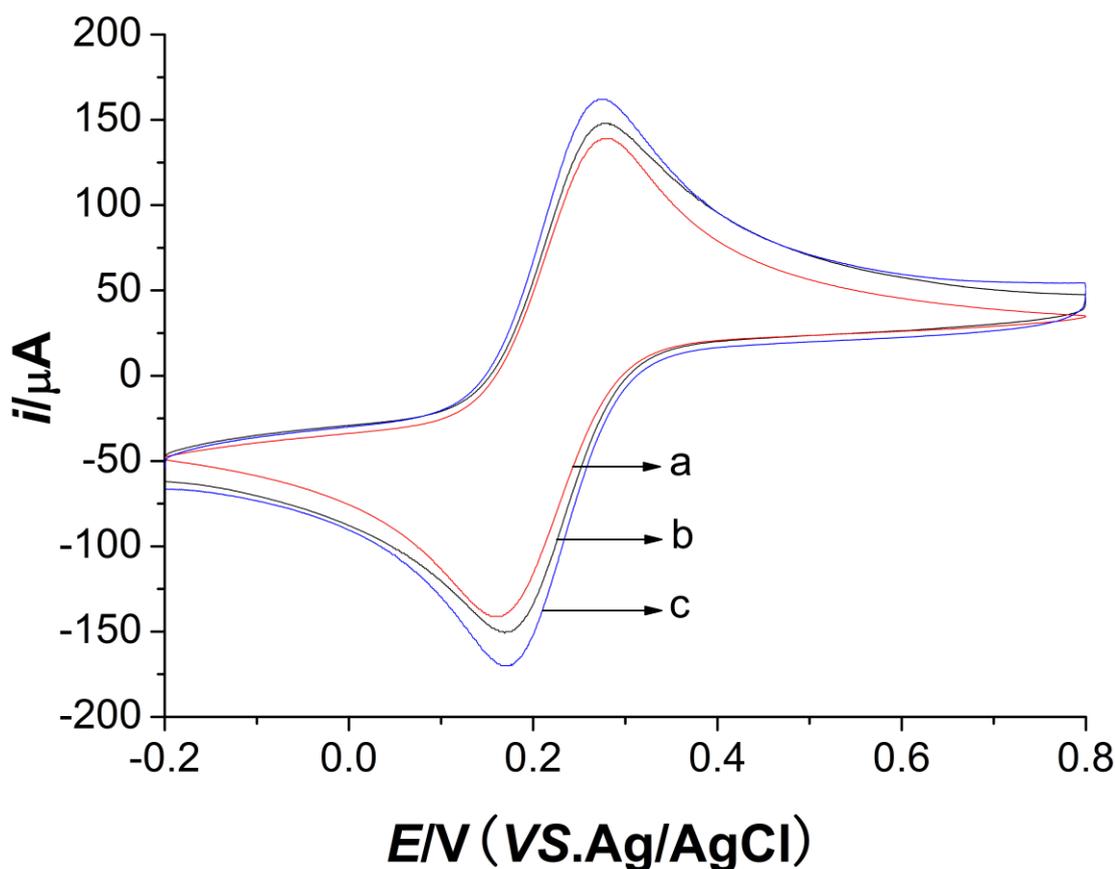

Figure 2. CVs of different electrode in 5.0 mmol·L^{-1} K$_4$[Fe(CN)$_6$]/K$_3$[Fe(CN)$_6$] (1:1) solution containing 0.1 mol·L^{-1} KCl: (a) GCE （b）MWCNTs/GCE （c）MWCNTs-COOH/GCE Scan rate: 100 mV·s^{-1}

3.2. Electrochemical behavior of Indole-3-carboxylic acid on different modified electrodes

Electrochemical behavior of 0.1 mmol·L^{-1} ICA on different modified electrodes was investigated in 0.2 mol·L^{-1} PP buffer solution (pH 6.5), which is shown in Fig. 3. Broad oxidation peak at 0.8-1.1 V is observed at bare GCE (curve a) which indicates a slow electron transfer. When MWCNTs are modified on the surface of GCE (curve b), the peak current of ICA can be significantly improved. The reason for the better performance of the MWCNTs/GCE could be attributed to the high

effective electrode surface area, electronic structure and structural defects presenting on MWCNTs surface [18, 19]. As clearly seen in curve c, the oxidation current obtained for ICA on the MWCNTs-COOH/GCE is much larger than that of MWCNTs/GCE or GCE. MWCNTs-COOH possesses high dispersion quality. The carboxylic acid group on the surface of MWCNTs can combine with the amino groups and carboxylic acid group of ICA via hydrogen bonds. So, the MWCNTs-COOH/GCE can absorb target molecules as much as possible. Based on the above reasons, the MWCNTs-COOH/GCE has strong enhancement ability for the electric signal of ICA.
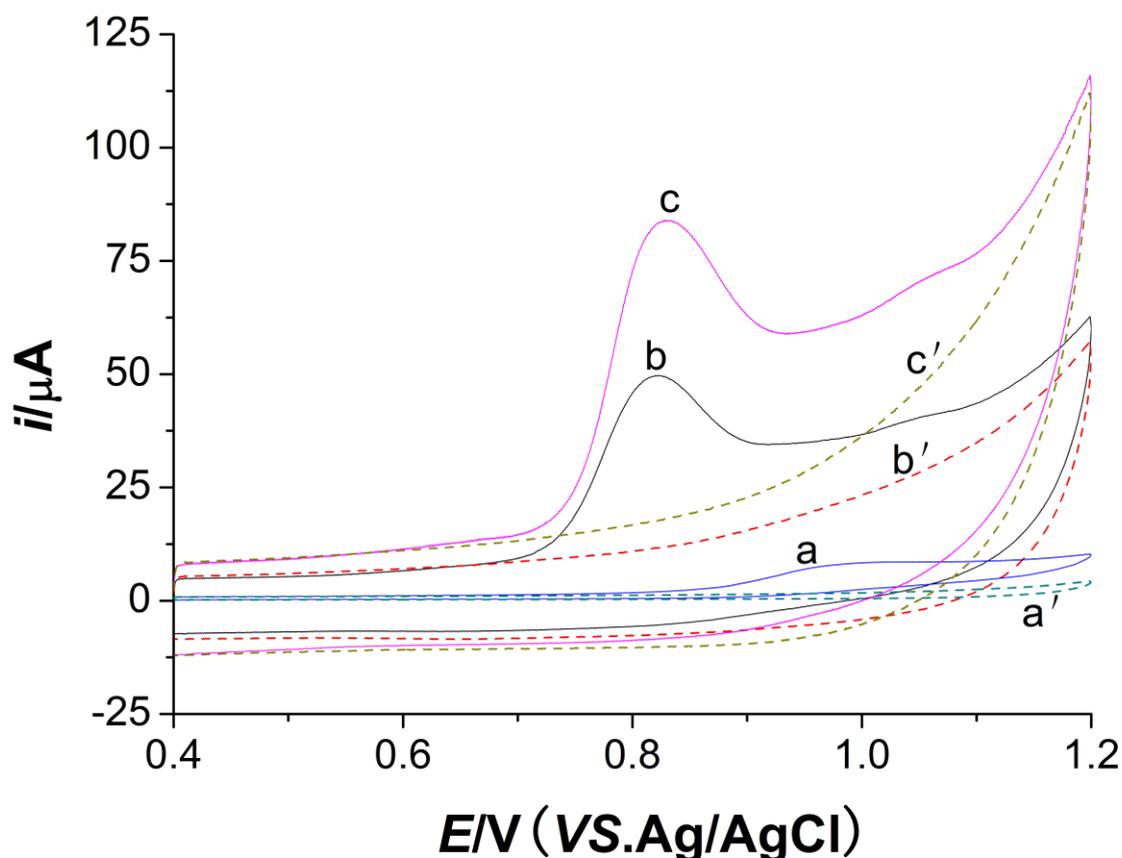
Figure 3. Cyclic voltammograms of 0.1 mmol·L^{-1} Indole-3-carboxylic acid in 0.2 mol·L^{-1} PP buffer solution at GCE(a), MWCNTs/GCE(b), MWCNTs-COOH/GCE(c). Dashed lines for GCE (a′), MWCNTs/GCE (b′) and MWCNTs-COOH/GCE (c′). pH: 6.5, Scan rate: 100 mV·s^{-1}, quiet time 270 s

3.3 Effect of accumulation time

Accumulation time can influence the absorption of ICA on the MWCNTs-COOH /GCE, and thus affects the determination sensitivity and detection limit. Therefore, the effect of accumulation time was investigated, which was shown in Fig.4. The oxidation peak current increases first when the time is accumulating, but it gradually decreases after it reaches the max value. The optimal accumulation time is 270 s. So an accumulation time of 270 s was employed in the subsequent experiments.
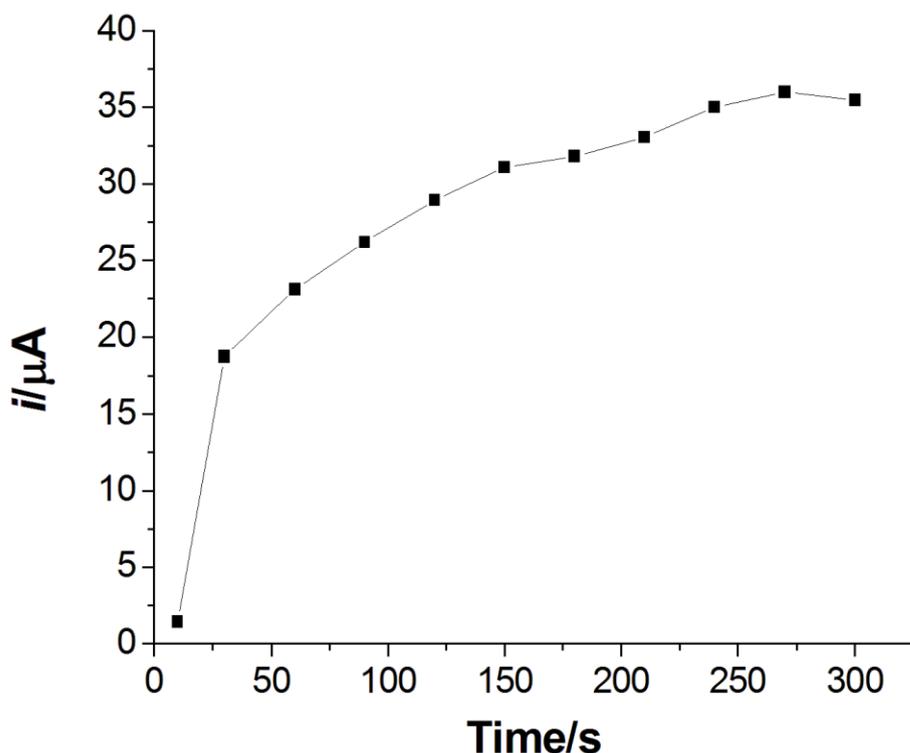
Figure 4. Different accumulation time of 0.1 mmol·L^{-1} ICA at MWCNTs-COOH /GCE in 0.2 mol·L^{-1} PP buffer solution.pH: 6.5, Quiet time: 10 s to 300 s, Applied potential: 100 mV vs. Ag/AgCl

3.4 Effect of varying volumes of MWCNTs-COOH

The volume effect of MWCNTs-COOH suspension was investigated to optimize the oxidation response of the MWCNTs-COOH/GCE for ICA by varying the volume from 5.0 to 25.0 μL. The oxidation peak current firstly increases and reaches its maximum value when 10 μL of 1.0 mg·mL^{-1} MWCNTs-COOH suspension was deposited on the surface of GCE. However, when the amount of the suspension exceeds 10 μL, the peak current conversely decreases. This is probably related to the thickness of the film.

In the process of increasing the modified dose, the increase of the active site on the surface of the electrode leads to the increase of peak current.

Too thin film would decrease the absorption of ICA. On the contrary, too thick film would make the conductivity of the electrode reduce and also make the film unstable as MWCNTs-COOH could leave off the electrode surface. Therefore, 10 μL of MWCNTs-COOH suspension was considered as an optimum amount to carry out sensitive determination of ICA.

3.5. The mechanism of ICA on the electrode

Fig. 5A exhibits the LSVs of ICA on MWCNTs-COOH/GCE with scan rate ranging from 40 to 1000 mVs^{-1} in 0.2 mol·L^{-1} PP buffer solution. At low scan rates, the oxidation peak is extremely weak

and broad. While at high scan rates, the oxidation peak appears and the oxidation peak current of ICA increases linearly with the increasing scan rate. These behaviors are consistent with the irreversible electrode process. The equation is $I_p = 0.0685\,v + 2.5203$ (R = 0.9972) (Fig. 5B). Based on the results, the oxidation of ICA at MWCNTs-COOH/GCE can be mainly ascribed to an adsorption-controlled process. An approximate estimate of the surface coverage of the electrode could be evaluated according to the equation [20, 21].

$$I_p = n^2F^2A\Gamma v/4RT$$

Where I_p is the peak current, n is the number of electrons involved, A is the surface area of the electrode (0.07065 cm^2), and v is the scan rate. R, T and F have their usual meanings which stand for the gas constant, the temperature and the Faraday constant, respectively. From the slopes of the linear plots of I_p *versus* v, the surface concentrations of electroactive species (Γ) can be calculated as 1.03×10^{-9} mol cm^{-2}.

For totally irreversible electrode process, E_p and v is defined by the following equation [22]:

$$E_{pa} = E^0 + (\frac{RT}{\alpha nF})\ln(\frac{RTk^0}{\alpha nF}) + (\frac{RT}{\alpha nF})\ln v$$

where E_{pa} is the oxidation peak potential (V), E^0 is the formal potential (V), α is the electron-transfer coefficient, k^0 is the standard rate constant of the surface reaction (s^{-1}), v is the scan rate (V s^{-1}), R, T and F are the gas constant, the temperature, and the Faraday constant, respectively. A linear correlation of E_{pa} *versus* $\ln v$ was obtained and their equation is $E_{pa} = 0.8575 + 0.0304\ln v$ (R = 0.9950). αn can be calculated as 0.85. According to Bard and Faulkner equation [23]:

$$\alpha = \frac{47.7mV}{E_P - E_{P/2}}$$

Where $E_{P/2}$ is the potential when the current is at half of the peak value. α can be calculated as 0.83. So the electron transfer number n is 1. One electron is involved in the oxidation of ICA.
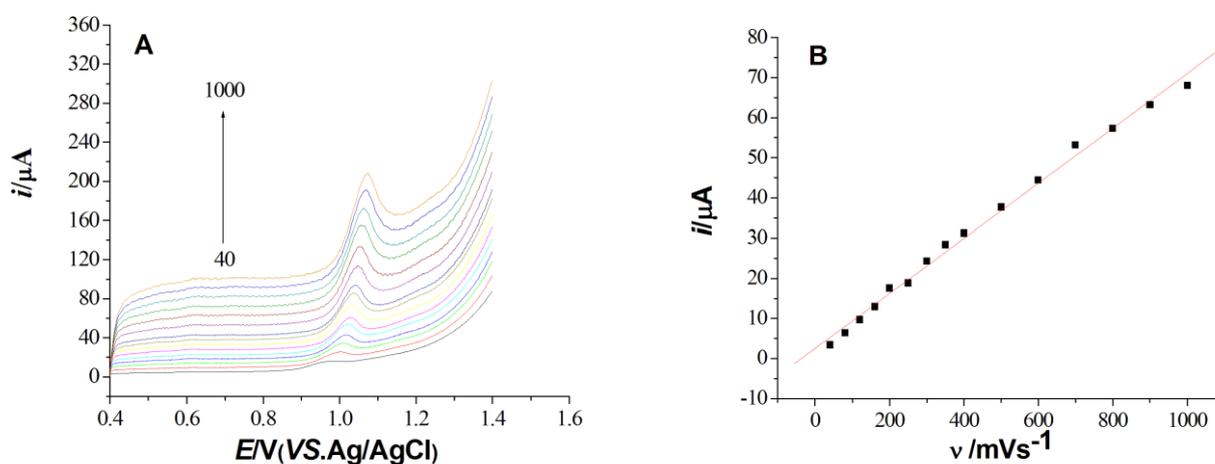
Figure 5(A). Effect of scan rate on the LSV of ICA with MWCNTs-COOH /GCE in 0.2 mol·L^{-1} PP buffer solution (pH 6.5) at scan rates of 40, 80, 120, 160, 200, 300, 350, 400, 500, 600, 700, 800, 900, 1000 mV s^{-1}. (B). plots of peak currents vs. the scan rates.
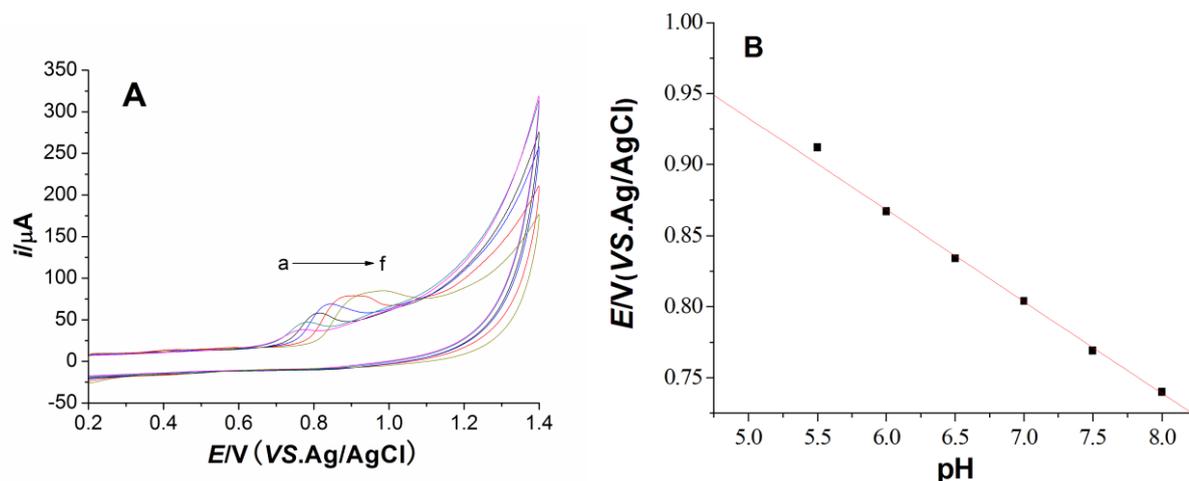
Figure 6(A). CVs of 0.1 mmol·L^{-1} ICA at MWCNTs-COOH /GCE in PP buffer solution with varied pH at a scan rate of 100 mV·s^{-1} and quiet time 270s.pH: a-8.0, b-7.5, c-7.0, d-6.5, e-6.0, f-5.5 (B). Plot of the potentials vs. the pHs.
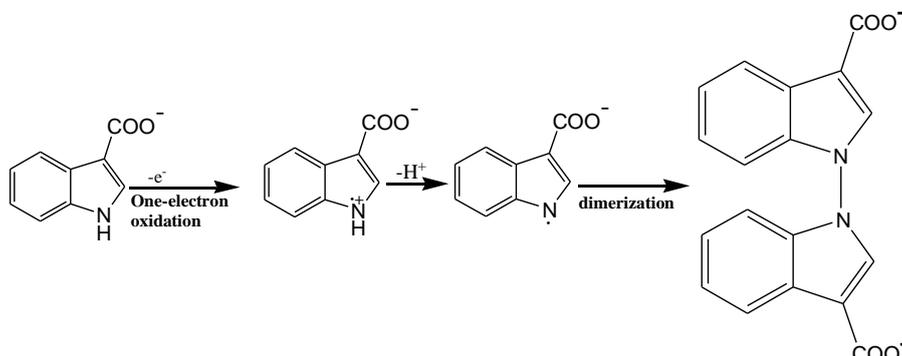

Figure 7. Possible mechanism of ICA on the MWCNTs-COOH /GCE.

The influence of pH on the electrochemical response of ICA at MWCNTs-COOH/GCE was studied in the range of 5.5-8.0 in 0.2 mol·L^{-1} PP buffer solution. As shown in Fig. 6A, a gradually negative shift of the peak potential is observed and the plot of the anodic peak potential *versus* pH value shows linearity in the pH range 5.5-8.0, which suggests that protons have taken part in their electrode reaction processes. The relationship between E_p and pH is E_p (V) = 1.2777 - 0.0677 pH (R = 0.9965) (Fig. 6B). The slope value (67.7 mV per pH unit) is close to the ideal value for a redox process involving electrons and protons in 1:1 ratio [24]. Obviously, the oxidation process of ICA is probably a one-electron and one-proton irreversible oxidation reaction. The possible mechanism of ICA on the MWCNTs-COOH/GCE is shown in Fig.7. In addition, the anodic peak current decreases gradually with increasing the pH of PP buffer solution, while the peak shape is abnormal with the pH less than 6.5. So the optimum pH 6.5 is chosen for the detection of ICA.

3.6 Calibration curve of IAA detection

DPV has a much higher current sensitivity than that of CV. The determination of ICA was performed at MWCNTs-COOH/GCE using DPV mode. Fig. 8 displays a series of solutions with varying ICA concentrations measured by DPV method under the optimal experimental conditions. The linear relationship between the concentration of ICA (C/μmol L^{-1}) and the oxidation peak current (I_{pa}/μA) can be described as $I_{pa} = 0.170 + 0.543$ C (R^2 = 0.9990). The linear response range of the sensor was 0.75–100 μmol L^{-1}, with the detection limit of 0.25 μmol L^{-1} (S/N = 3), suggesting that this sensor exhibits a relatively good sensitivity to ICA.
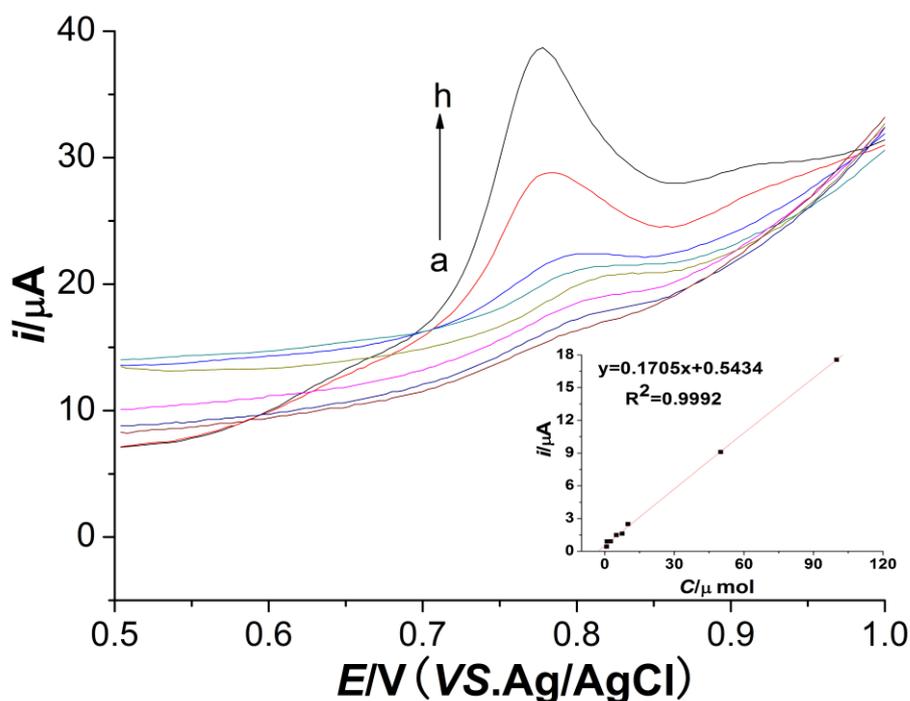
Figure 8. DPV responses for ICA of varied concentrations in the range of 0.75-100 μmol L^{-1} at MWCNTs-COOH /GCE in 0.2 mol L^{-1} PP buffer solution (pH 6.5). Inset: corresponding linear calibration curve of peak current versus ICA concentration.Various concentrations of ICA(a→h): 0.75,1.0,2.5,5.0,7.5,10.0,50.0,100.0 μmol·L^{-1}.

3.7 Selectivity, repeatability and stability

The interferences from several organic compounds with similar structures and some conventional inorganic ions were studied separately for the determination of ICA using the modified electrode was evaluated. The results show that ascorbic acid, histidine, tryptophan, Na$^+$, Ca^{2+}, Mg^{2+}, SO$_4^{2-}$, Cl$^-$ in 100 fold of ICA concentration do not affect the detection signals generated by ICA. The selectivity of the ICA sensor seems satisfactory.

The repeatability of the sensor was examined by successive nine detections of 10 μmol L^{-1} ICA at a single modified electrode. The relative standard deviation (RSD) in peak currents was 5.6%,

suggesting that the electrode has excellent repeatability.

The stability was investigated by taking measurements of 10 μmol L^{-1} ICA during seven consecutive days using the same electrode. The modified electrode was stored at ambient temperature. All measurement results obtained fell in the range of 92.6 – 108.3% of its initial current response. The results show that the here present modified electrode has good stability.

As compared with similar sensors for the determination of ICA (Table 1) in the previous reports, improved or comparable performance for the determination of IAA can be achieved using the MWCNTs-COOH/GCE. In addition, a relatively wide linear range and low detection limit can be obtained by using modified electrode, although IAA is more difficult to be oxidized than ICA.

Table 1. Comparison of similar sensors for IAA or ICA determination

Electrode materials	Detected compounds	Linear range (μmol·L-1)	LOD (μmol·L-1)	References
PST-rGO	ICA	0.1-7.0	0.05	5
HeminE	ICA	2-400	0.025	25
PEDOTM/GO	ICA	0.6-10	0.087	26
MWNT-DHP	ICA	0.1-50.0	0.02	27
Graphite-polyurethane	ICA	1.3-94.7	0.15	28
MWNT/MPS/Pt	ICA	1-20	0.1	29
MWCNTs-COOH	IAA	0.75-100	0.25	This work

3.8. Determination of IAA in real sample (cabbage samples)

The applicability of proposed sensor was assessed by the determination of ICA concentration in cabbage leaves. The procedure of treating the sample was as follows: 100 g of cabbage leaves was treated with liquid nitrogen and then pulverized. The compound was extracted with ethyl acetate and separated by an extraction method [30]. After extraction, the remainder was dissolved in 5 mL methanol. The mixture was transferred to a flask and then diluted with distilled water to 50 mL. Sample detection was carried out and the recovery experiments were designed by adding ICA standard solution in samples. Each measurement was replicated for five times. The results were shown in Table 2. Concentration of ICA detected by proposed sensor is 3.97 μmol·L^{-1}. The average recoveries ranged between 90.8% and 101.3%, and the RSDs are less than 5.3% (n = 5). The sample was also detected by

HPLC method. The average concentration of ICA was $3.65\,\mu mol \cdot L^{-1}$. The results obtained by HPLC and IAA sensor are very close, indicating that the proposed method has potential for applicability for the detection of ICA in real samples.

Table 2. Determination results of ICA in cabbage leaves

Compound	Detected ($\mu mol \cdot L^{-1}$)	Added($\mu mol \cdot L^{-1}$)	Found($\mu mol \cdot L^{-1}$)	Recovery (%)	RSD (%)
ICA	3.97	5	8.51	90.8	5.3
		50	54.63	101.3	4.2

4. CONCLUSIONS

In this paper, a rapid, simple and highly sensitive method for the electrochemical determination of ICA was developed. This satisfied analytical performance should be attributed to MWCNTs-COOH modified electrode with high electrocatalytic activity and high sensitivity for ICA. The biosensor shows large linear working range of $0.75–100$ μmol L^{-1}, low detection limit of 0.25 μmol L^{-1}, furthermore, by which ICA in real samples was determined successfully.

References

1. G. Sandberg, E. Jensen and A. Crozier, *Phytochemistry.*, 23 (1984) 99.
2. J. MacMillan, PEncyclopedia of Plant Physiology, Springer-Verlag, (1980) New York, America.
3. O. Sagee, J. Riov and R. Goren, *Plant Physiol.*, 91 (1990) 54.
4. M. Wurst, Z. Přikryl and J. Vokoun, *J. Chromatogr. A*, 286 (1984) 237.
5. T. Gan, C. G. Hu, Z. L. Chen and S. S. Hu, *Talanta.*, 85 (2011) 310.
6. Z. L. Feng, Y. Y. Yao, J. K. Xu , L. Zhang, Z.F. Wang and Y. P. Wen, *Chin. Chem. Lett.*, 25 (2014) 511.
7. Y. L. Zhou, Z. N. Xu, M. Wang, X. M. Meng and H. S. Yin, *Electrochim. Acta*, 96 (2013) 66.
8. J. P. Li, W. L. Yin, Y. J. Tan and H. C. Pan, *Sensors and Actuators B.,* 197 (2014) 109.
9. E. Canbay and E. Akyilmaz, *Anal. Biochem.*, 444 (2014) 8.
10. G. Y Xu, B. B. Li, X. Y. T. Cui, L. Y Ling and X. L. Luo, *Sensors and Actuators B.,* 188 (2013) 405.
11. A. T. EzhilVilian, S. M. Chen and B.S. Lou, *Biosens. Bioelectron.*, 61 (2014) 639.
12. J. Liu, A. G. Rinzler, H. J. Dai, J. H. Hafner, R.K. Bradley, P.J. Boul, A. Lu, T. Iverson, K. Shelimow, C.B. Huffman, F. Rodriguez-Macias, Y.S. Shon, T.R. Lee, D.T. Colbert and R.E. Smalley, *Sci.,* 280 (1998) 1253.
13. D. Lahiri, S. Ghosh and A. Agarwal, Mater. Sci. Eng., C, 32 (2012) 1727.

14. T. Hasan and G. Hosna, *C.R. Chim.*, 16 (2013) 838.
15. S. K. Zhu and X. L. Su, *J. Anal. Sci.*, 28 (2012) 775.
16. W. Sun, Y. H. Wang, S. X. Gong, Y. Cheng, F. Shi and Z. F. Sun, *Electrochim. Acta.*, 109 (2013) 298.
17. F. Sundfors, J. Bobacka, A. Ivaska and A. Lewenstam, *Electrochim. Acta.*, 47(2002) 2245.
18. E. Katz, I. Willner and J. Wang, *Electroanalysis.,* 16 (2004)19.
19. H. Xiong, Y. Zhao, P. Liu, X. Zhang and S. Wang, *Microchim. Acta.*, 168 (2010) 31.
20. A. P. Brown and F. C. Anson, *Anal. Chem.*, 49 (1977) 1589.
21. M. Sharp, M. Petersson and K. Edström, J. Electroanal. Chem., 95 (1979) 123.
22. E. Laviron, J. Electroanal. Chem., 52 (1974) 355.
23. A. J.Bard and L. R. Faulkner, Electrochemical methods fundamentals and application (2nd ed.), Wiley, (2004) New York, America.
24. S. Shahrokhian, M. Galkhani, M. Adeli and M.K. Amini, *Biosens. Bioelectron.*, 24 (2009) 3235.
25. G. N. Chen, Z. F. Zhao, X. L. Wang, J. P. Duan and H. Q. Chen, *Anal. Chim. Acta*, 452 (2002) 245.
26. Z. L. Feng, Y. Y. Yao, J. K. Xu, L. Zhang, Z. F. Wang and Y. P. Wen, Chinese Chemical Letters, 25 (2014) 511.
27. K. B. Wu, Y. L. Sun and S.S. Hu, Sens. *Actuators B: Chem.*, 96 (2003) 658.
28. R.A. de Toledo and C.M.P. Vaz, *Microchem J*, 86 (2007) 161.
29. S. Mancuso, A.M. Marras, V. Magnus, et aL, and F. Baluškad, *Anal. Biochem.*, 341 (2005) 344.
30. P. Hernández, F. Galán, O. Nieto and L. Hernández, *Electroanalysis.*, 6 (1994) 577.